Shear Work and Liquefaction Resistance of Crushable Pumice Sand

Rolando P Orense[1][0000-0002-0581-9563], Jenny Ha[1], Arushi Shetty[1] and Baqer Asadi[2][0000-0001-8191-3757]

[1] University of Auckland, Auckland 1142, New Zealand
[2] Jacobs, Auckland, New Zealand
r.orense@auckland.ac.nz

Abstract. Crushable volcanic soils, such as pumice sands, are often encountered in engineering projects in the North Island of New Zealand. Due to the highly crushable nature of the pumice sand components, current empirical correlations, derived primarily from hard-grained sands, are not applicable when evaluating the liquefaction potential of pumice-rich soils. To better understand their liquefaction characteristics, cyclic undrained triaxial tests were performed on high-quality undisturbed soil samples sourced from various pumice-rich sites in the North Island. The undrained response, expressed in terms of the development of excess pore water pressure and axial strain with the number of cycles, and the shear work (or cumulative dissipated energy), defined as the energy consumed by the soil during plastic deformation until liquefaction, is examined vis-à-vis the pumice contents of the specimens. When compared to published trends for normal sands available in the literature, the results indicate that the shear work for pumice-rich sands sand is larger in specimens with higher pumice contents because some energy is spent as the particles undergo crushing. As a result, the liquefaction resistance of crushable pumice sand is higher than that of natural sand for the same level of loading applied.

Keywords: Liquefaction, Pumice sand, Cyclic test, Shear work, Particle crushing.

1 Introduction

Pumice deposits are found in several areas of the North Island of New Zealand. They originated from a series of volcanic eruptions centred in the Taupo and Rotorua regions, called the "Taupo Volcanic Zone". While they exist mainly as deep sand layers in river valleys and flood plains, they are also found as coarse gravel deposits in hilly areas. As a result, they are often encountered in engineering projects being undertaken in the region.

These deposits contain pumice sands, characterised as lightweight, highly crushable, and compressible due to their vesicular nature. SEM imaging indicates that pumice sands have lots of surface and internal voids (see Fig. 1a). The single-particle

crushing strength of pumice sand is one order of magnitude less than normal silica sand (see Fig. 1b); it can be crushed by fingernail pressure. Cone penetration tests on loose and dense pumice sand deposits in a CPT chamber showed that the cone resistance profile is practically the same for both density states, presumably due to particle crushing when the rod penetrates the deposit (see Fig. 1c). The results indicate that cone resistance is not an appropriate index to represent the relative density of soil.

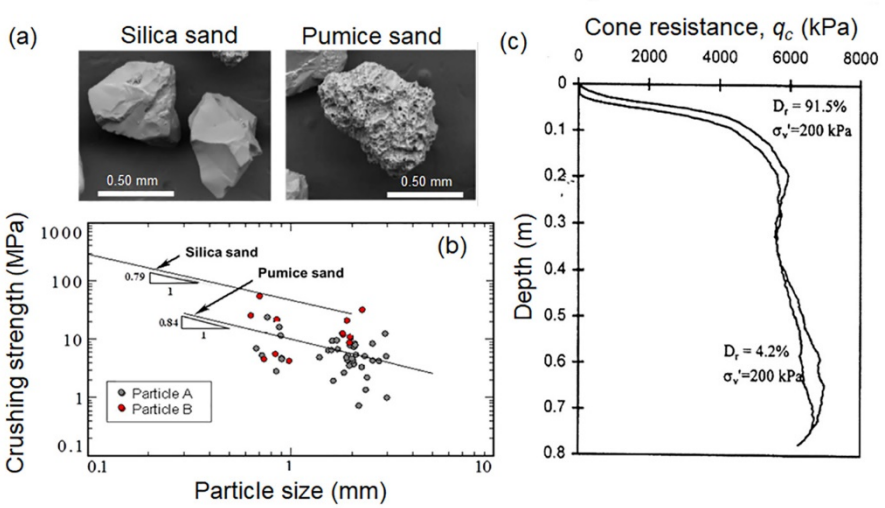

Fig. 1. Comparison between silica sand and pumice sand in terms of: (a) particle characteristics from SEM images; (b) single particle crushing strength as a function of particle size [1]); and (c) cone penetration resistance in chamber test [2]).

Because of the presence of these crushable pumice sands in the soil matrix, laboratory undrained cyclic triaxial tests conducted at the Geomechanics Laboratory (University of Auckland) showed that pumiceous sands behave differently when compared to normal (hard-grained) silica sands [3-5]. Hence, conventional methods of estimating the liquefaction resistance of soils in the field do not apply to these materials.

To better understand their liquefaction characteristics, high-quality soil samples were obtained from various pumice-rich sites in the North Island using diverse sampling techniques and then tested in the laboratory using a cyclic triaxial apparatus. Moreover, the pumice content of each sample was quantified using a recently developed method that correlates the degree of particle crushing of the samples to the amount of crushable pumice particles present. In addition to the undrained response, expressed in terms of the development of excess pore water pressure and axial strain with the number of cycles, and the shear work (or cumulative dissipated energy), defined as the energy consumed by the soil during plastic deformation until liquefaction, was also examined.

The cumulative dissipated energy, ΣW, is indicated by the area under the deviator stress and axial strain (see Fig. 2a). It represents the energy consumed by the soil

during plastic deformation until liquefaction, and therefore a good indicator of the cyclic shear behaviour and liquefaction strength of the soil.

2 Materials used and Methodology

2.1 Samples investigated

High-quality undisturbed pumice-rich samples were obtained from six sites within the Waikato Basin and Bay of Plenty region in the central part of North Island. These samples were obtained using the Dames & Moore (DM) sampler and the Gel-push sampler (both triple-tube type, GPTR, and static type, GPS). The index properties of the samples obtained are reported by Asadi et al. [6], while details about the undisturbed soil sampling methods are discussed by Stringer [7].

2.2 Quantification of Pumice Content

The pumice-rich sands collected from various sites showed different amounts of pumice particles present in the soil mixture. To estimate the pumice content (*PC*), defined as the ratio (by weight) of the amount of the crushable pumice sand components to the total amount of the sample, the methodology developed by the authors [8-9] was followed. According to this approach, which is based on the crushability feature of the pumice sands, the *PC* of the specimens are estimated based on the relative breakage, B_r, measured during a modified maximum dry density (MDD) test. The relation between PC and B_r is illustrated in Fig. 2b.

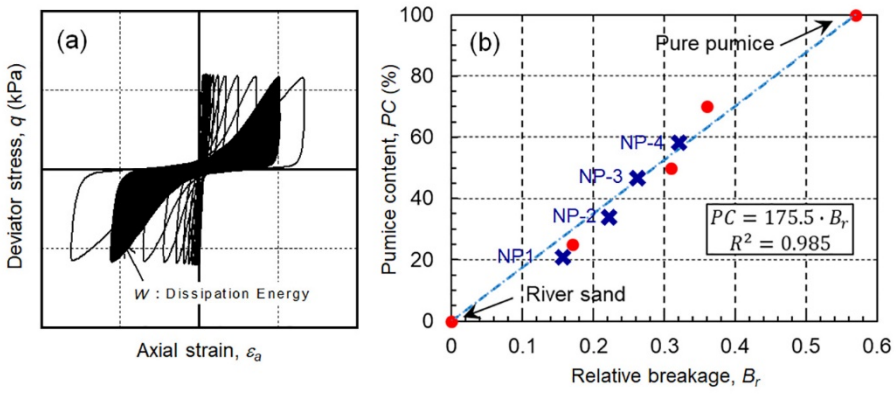

Fig. 2. (a) Schematic diagram of cumulative dissipated energy, ΣW; (b) Relation between pumice content and relative breakage from Modified MDD test [8-9].

2.3 Testing Programme

Overall, 21 undisturbed soil samples from 6 locations were tested in the laboratory. The majority of the samples were tested three times (although some were tested 2-6

times) under different levels of cyclic shear stress ratio (*CSR*). All tests were conducted under an effective confining pressure σ'_c=100 kPa and a loading frequency f=0.1 Hz. A summary of the laboratory undrained cyclic triaxial tests performed is presented in Table 1, including the range of pumice contents and samplers used. For each test, the development of double amplitude axial strain, ε_{DA}, and excess pore water pressure ratio, r_u (=u/σ'_c, where u is the excess pore water pressure) with the number of cycles were obtained. For each test, the shear work per cycle was calculated from the deviator stress-axial strain curves using MATLAB.

Table 1. Summary of laboratory tests conducted

Location ID	No. of samples	No. of tests/ sample	Pumice content (%)	Sampler used
Tauranga 1	5	3	72, 72, 19, 19, 40	DM (×5)
Tauranga 2	3	3	0, 45, 43	GPTR (×3)
Hamilton – GS	3	2-4	35, 93, 93	DM (×1), GPTR (×2)
Hamilton – TR	2	2-3	16, 38	GPTR (×1), DM (×1)
Edgecumbe	3	3-4	36, 42, 39	GPTR (×3)
Whakatane	5	2-6	71, 35, 38, 88, 55	GPS (×1), DM (×1), GPTR (×2)

3 Results and Discussion

3.1 Development of axial strain and pore water pressure with cyclic loading

To examine the undrained cyclic behavior of pumice-rich sands, the maximum values of ε_{DA} and r_u at the end of each loading cycle are plotted versus the normalised number of cycles in Figs. 3 and 4, respectively. In the figure, the number of cycles, N, was normalised by N_{liq}, defined as the number of cycles required to reach ε_{DA}=5%. The plots shown correspond to tests with roughly similar *CSR*. For the purpose of the analysis, the samples were grouped into three broad pumice content ranges such that bias in individual specimens was reduced and general trends could be observed: zero (*PC*=0%), low (*PC*=16~35%) and high (*PC*=72~93%) pumice contents.

From both figures, while there is a general scatter of results (due to the undisturbed samples having different relative densities, fines contents, fabric/structure, stress history, etc.), a general trend of the plots can be observed: (1) Specimens with low pumice content (*PC*=0%) show negligible deformation during the early part of the cyclic load application, although some development in pore water pressure occurred. During the middle-third of the loading, the rate of increase in r_u decreases; however, when it reaches a specific value, an immediate increase in r_u is generated, accompanied by a sudden occurrence of large deformation, leading to liquefaction in just a few cycles. (2) Specimens with high pumice content ((*PC*=72~93%) show a similar immediate increase in r_u at the initial stage of loading, but with almost twice the rate of r_u development; moreover, the initial deformation is much higher. In the next stage, the rate

of increase in r_u decreases gradually until initial liquefaction (i.e., where the specimen reached $r_u > 0.95$) is reached. They also show a gradual increase in deformation, starting from the beginning of the cyclic loading and steadily increasing until liquefaction, in an almost linear fashion, due to particle crushing. Note that these specimens can undergo large deformation even under high r_u, presumably because of the formation of a more stable soil skeleton induced by crushing. (3) Specimens with low pumice content ((*PC*=16~35%) show deformation and pore pressure responses that are midway between the zero and high *PC* specimens.

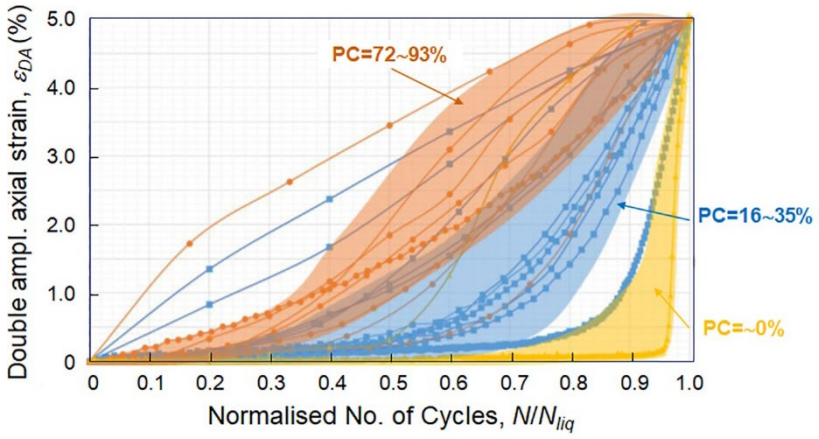

Fig. 3. Relation between double amplitude axial strain and normalised number of cycles for pumice-rich samples with different pumice contents.

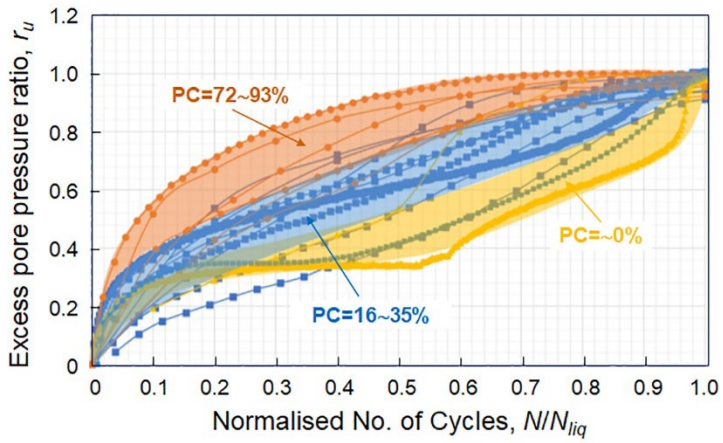

Fig. 4. Relation between excess pore water pressure ratio and normalised number of cycles for pumice-rich samples with different pumice contents.

3.2 Development of cumulative dissipated energy with cyclic loading

As discussed earlier, the dissipated energy per cycle is calculated as the area within each hysteresis loop. Due to the increasing strain caused by an increase in the excess pore water pressure, these loops typically increase in area with an increase in the number of cycles. Fig. 5 plots the development of the cumulative dissipated energy for specimens in the three *PC* ranges. For zero *PC* specimens, the initial development of ΣW is very slow because of the very minimal amounts of strain the specimens experienced. As the number of cycles increases towards liquefaction, the axial strain begins to increase in much larger increments, resulting in a significant increase in ΣW. On the other hand, specimens with high *PC* tend to have greater cumulative dissipated energy, even at the start of the cyclic load application.

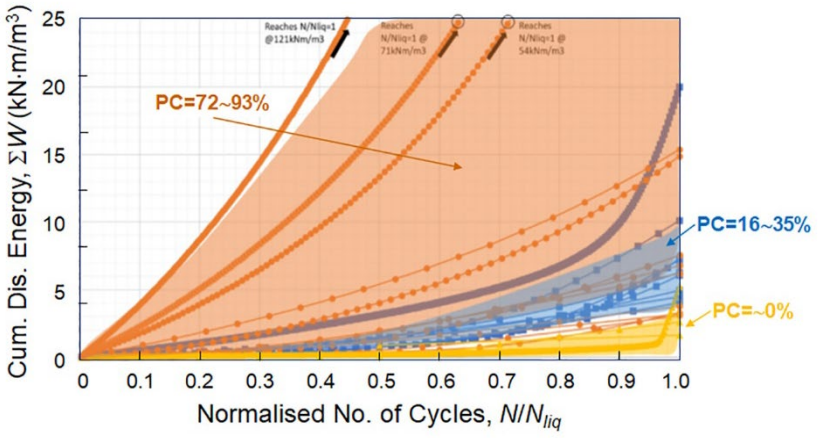

Fig. 5. Relation between cumulative dissipated energy and normalised number of cycles for pumice-rich samples with different pumice contents.

3.3 Development of deformation and pore pressure with shear work

To observe clearly how the axial deformation and excess pore water pressure vary with the cumulative dissipated energy, the median curves of the trends of each of the above parameters with the normalised number of cycles (i.e., Figs. 3-5) for each *PC* range are obtained and plotted with respect to each other; these are shown in Fig. 6. Also shown in the figures are trends for the natural sand materials (with relative density D_r=50%) reported by Yoshimoto et al. [10]. Based on Fig. 6a, ΣW of zero *PC* sand is similar to the other hard-grained sands, while that of medium *PC* sands is about 2-4 times higher than those of natural sands and almost the same as that of Iwakuni clay. Finally, the ΣW of high *PC* specimens is nearly one order of magnitude greater than those of normal sands. The same trends are presented in Fig. 6b in terms of the relation between ΣW and r_u. Normal sands are not resistant to liquefaction because they lack energy absorption capacity. In contrast, r_u in Iwakuni clay increases only up to about 0.6 when ε_{DA}=5%. It is also observed that natural sands and pumice-

rich show similar behaviour until r_u=0.6; however, in the case of high *PC* specimens, r_u does not reach 1.0 when ε_{DA}=5%. Based on the trends, pumice-rich sands are more resistant to liquefaction than natural sands, possibly because some energy is dissipated as the particles crush due to cyclic loading.

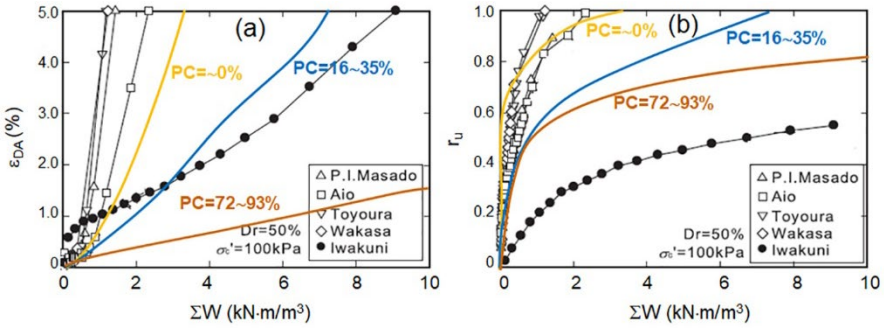

Fig. 6. Comparison of the development of: (a) double amplitude axial strain; and (b) excess pore water pressure ratio with cumulative dissipated energy for representative pumice-rich samples (with varying pumice contents) and normal (hard-grained) sands.

3.4 Comparison of liquefaction resistance curves

To illustrate the higher liquefaction resistance of pumice-rich sands, representative samples for each *PC* range are selected and plotted in Fig. 7, together with those of natural sands [10]. Although these pumiceous sand specimens are from undisturbed samples (with different relative densities, fines contents, fabric/structure, degrees of cementation, etc.) while the natural sand specimens are reconstituted, a general trend is observed: zero *PC* sand has the same the liquefaction resistance as ordinary sands, while low *PC* and high *PC* sands have higher liquefaction resistance.

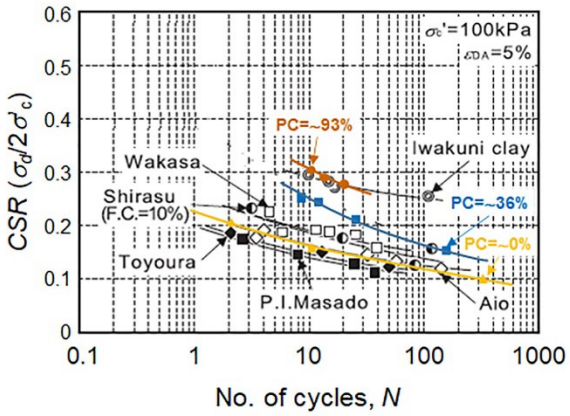

Fig. 7. Comparison of liquefaction resistance curves of representative pumice-rich samples (with varying pumice contents) and normal (hard-grained) sands.

4 Concluding Remarks

The results of undrained cyclic triaxial tests conducted on high-quality undisturbed sand samples with varying pumice contents (*PC*) were analysed. It was observed that under cyclic loading, samples with high *PC* have a greater cumulative dissipated energy response than those with low and zero *PC*. This could be attributed to particle crushing and subsequent stabilisation of pumice soil structure, manifested in a greater initial build-up of r_u and larger deformations. The presence of some amount of crushable pumice sand in the sample resulted in higher cumulative dissipated energy and greater liquefaction resistance than normal sands. Note that other factors, such as particle size, fines contents, fabric/structure, cementation and stress history, etc., may also have varying effects on the observed response.

Acknowledgment

Parts of this project were funded by the Natural Hazards Research Platform (NHRP) and QuakeCoRE, a New Zealand Tertiary Education Commission-funded Centre. This is QuakeCoRE Publication Number 0730.

References

1. Orense, R.P., Pender, M.J., Hyodo, M., Nakata, Y. Micro-mechanical properties of crushable pumice sands. Géotechnique Letters, 3, Issue April–June, 67–71 (2013).
2. Wesley, L. D., Meyer, V. M., Pronjoto, S., Pender, M. J., Larkin, T. J., Duske, G. C. Engineering properties of pumice sand. 8th ANZ Conf. Geomechanics, 2, 901–908 (1999).
3. Orense, R.P., Pender, M.J. "Liquefaction characteristics of crushable pumice sand," 18th Int. Conf. Soil Mechanics & Geotechnical Engineering, 1, 1559-1562 (2018).
4. Orense, R.P., Asadi, M.S., Asadi, M.B., Pender, M.J., Stringer, M.E. "Field and laboratory assessment of liquefaction potential of crushable volcanic soils," Theme Lecture, 7th Int. Conf. Earthquake Geotechnical Engineering, 442-460 (2019).
5. Orense, R.P., Asadi, M.B., Stringer, M.E., Pender, M.J. Evaluating liquefaction potential of pumiceous deposits through field testing: Case study of the 1987 Edgecumbe earthquake. Bull. New Zealand Society for Earthquake Engineering 53(2), 101-110 (2020).
6. Asadi, M.B., Orense, R.P., Asadi, M.S., Pender, M.J. (2021). Experimental and simplified correlations for liquefaction assessment of crushable pumiceous sand by shear wave velocity. J. Geotech. & Geoenv. Engg. (submitted). (2021).
7. Stringer, M., Taylor, M., and Cubrinovski, M. Advanced soil sampling of silty sands in Christchurch." Report No: 2015-06, University of Canterbury: Christchurch, NZ. (2015).
8. Asadi, M.S., Orense, R.P., Asadi, M.B., Pender, M.J. Maximum dry density test to quantify pumice content in natural soils. Soils and Foundations, 59(2), 532-543 (2019).
9. Asadi, M.S., Orense, R.P., Asadi, M.B., Pender, M.J. (2021). Laboratory-based method to quantify pumice contents of volcanic deposits. 6th Int. Conf. Geotech. & Geophysical Site Characterization, Budapest, Hungary (2021).
10. Yoshimoto, N., Orense, R., Hyodo, M. & Nakata, Y. Dynamic behaviour of granulated coal ash during earthquakes. J. Geotech. & Geoenv. Engg, 140(2), 0413002 (2014).